ELSEVIER

Chemical Engineering Journal 70 (1998) 157–163

Chemical Engineering Journal

Short communication

Pyrolysis of automotive shredder residues: a lumped kinetic characterization

Oreste Patierno [a], Paola Cipriani [a], Fausto Pochetti [a], Massimiliano Giona [b,*]

[a] *Dipartimento di Ingegneria Chimica, Universitá di Roma 'La Sapienza', via Eudossiana 18, 00184 Roma, Italy*

[b] *Dipartimento di Ingegneria Chimica, Universitá di Cagliari, piazza d'Armi, 09123 Cagliari, Italy*

Received 28 April 1997; revised 6 November 1997; accepted 7 December 1997

Abstract

A lumped kinetic model for the pyrolysis of industrial wastes of unknown chemical composition is developed. The model is applied to the pyrolysis of automotive shredder residues (ASRs), studied by means of thermogravimetric and calorimetric analyses, in isothermal and non-isothermal conditions.

Keywords: Pyrolysis; Thermal treatment; Industrial wastes; Lumped kinetic models; ASRs

1. Introduction

Thermochemical treatment (pyrolysis, gasification, etc.) of complex organic materials is one of the most promising methods for the reduction of the impact of solid, municipal and industrial wastes as it regards environmental issues, storing and landfilling costs, and can also be used to produce energy [1]. Research on the pyrolysis and gasification of wastes has increased significantly in the last 10 years as a consequence of the increased importance of environmental issues and pollution; it can be used to recycle solid wastes with the benefit of a net energy gain.

The design of waste gasifiers and pyrolytic reactors requires the understanding and quantitative modelling of thermal decomposition kinetics. The kinetics of pyrolysis in the treatment of solid wastes is not only interesting in itself (e.g., in the design of flash pyrolytic reactors [2]), but also in the design of combustor and gasifier units. Indeed, at the inlet of a gasifier, poor mixing conditions, low oxygen concentration and low heating rates occur, thus promoting the pure thermal decomposition of the material [3].

The literature on the kinetics of pyrolysis of organic wastes has been mainly focused on cellulose (and its derivatives) [1,4–6], wood [7–9] and refuse-derived fuel (RDF) [3,10].

Cellulose represents a consistent fraction of urban wastes, and the overall pyrolytic kinetics of biomass is strongly influenced by the presence of cellulose components [1]. Accurate kinetic analyses of the thermal decomposition of cellulose have been performed experimentally and theoretically. Amongst the kinetic models developed, the models of Broido and Nelson [4] and Shafizadeh [5] are particularly worth attention, because these schemes influence strongly the modelling of more complex materials.

RDF is another material suitable for pyrolysis and gasification. It is obtained by converting the combustible fraction of urban solid wastes into fuel. In spite of the fact that RDF is a heterogeneous material, its chemical composition can be characterized in a fairly accurate way, and is practically constant (although significant composition variations in RDF occur from country to country). Indeed, within a single country, RDF contains an almost constant proportion of wood, polyethylene and α-cellulose [10].

In the case of cellulose, wood and RDF, the chemical composition is known, and this simplifies considerably the development of kinetic schemes, because it is possible to study separately the thermal decomposition kinetics of each principal compound.

However, there are many types of industrial waste the chemical composition of which is unknown, and the thermal treatment of which is highly desirable to reduce their environmental impact.

In this paper, we study the pyrolysis kinetics of automotive shredder residues (ASRs), also referred to as auto fluff [11], by means of a semiempirical lumped model. ASRs are highly heterogeneous, complex solid mixtures, containing plastics, foams, rubber, glass (silica), moisture, metals and metal

* Corresponding author.

PII S1385-8947(98)00072-2

Table 1
Chemical analysis (wt.%, dry basis) compared with the data of Shen et al. [11] on Canadian ASRs

Element	C	H	N	O	S	Cl	Other
Our data	17.5	2.10	0.53	17.42	0.25	0.05	62.15
Data by Shen et al. [11]	27.9	4.0	0.9	17.0	0.3	0.5	25.2 (Fe_2O_3), 18.5 (SiO_2^-)

oxides. ASRs are obtained from the demolition of vehicles during the recovery of the principal metallic parts.

The thermal treatment of such a biomass displays several advantages: (1) a reduction in storing and/or landfilling problems; (2) the elimination of metal ions and metal compounds which may cause the pollution of water basins; (3) the production of energy.

Due to the highly heterogeneous nature of ASRs, very little is known about this thermal decomposition kinetics; recently, preliminary attempts have been made to model the ultrapyrolytic processes of ASRs [11].

The aim of this study is to analyse, in some detail, the pyrolysis kinetics of ASRs. Attention is focused mainly on the lumped characterization of the weight loss kinetics with time, under a broad range of experimental (isothermal and non-isothermal) conditions, starting from thermogravimetric experiments.

In the pyrolysis of ASRs, the kinetic model must face the problem that a detailed chemical characterization of the material (such as for RDF [10]) is not available. Therefore, very refined models, which include nonlinear kinetics (see, for example, Refs. [7,8,12]) should be discarded, unless motivated by striking experimental evidence (see Ref. [13] for a discussion).

For this reason, linear reaction rates are assumed throughout this study, and it is shown in Section 4 that this assumption is in satisfactory agreement with experimental (isothermal) data.

The article is organized as follows. Section 2 describes the material properties and the experimental set-up. Section 3 develops the lumped kinetic analysis, and Section 4 discusses the experimental results and the comparison with the model proposed.

2. Materials and experimental set-up

2.1. Materials

ASRs were obtained from an automobile residue recycling plant, Ecofer, near Rome, Italy. This plant treats about 150×10^3 kg h^{-1} of residues, separating ferrous from non-ferrous materials. Approximately 20 wt.% of initial material is non-ferrous and, of this, 7–8 wt.% is metallic residue (copper, aluminium, etc.). Materials, once shredded, are treated in a depulveretor to remove light components, such as wood powders, tissue and light rubber fragments, etc. This operation is performed in a pipe, in the presence of a countercurrent air flow, which removes light materials via a cyclone in which separation is performed by this air flow.

The material coming from a single shredder displays a very narrow range of variation in composition. Elemental chemical analysis of ASRs was performed; the results are shown in Table 1, compared with the data of Shen et al. [11] for Canadian ASRs. As can be observed, the ASRs under consideration display a significant amount of metallic and silica residues, much higher than the material analysed in Ref. [11], and a smaller carbon content.

Before pyrolysis, the ASRs were shredded and ground to 0.5 mm, and dried in a furnace for 3 h at 115°C. The weight loss after drying was about 3.4 wt.%. In spite of the drying procedure, a small amount of moisture and/or bond-water is still present in the sample due to its exposure to atmospheric conditions for a short period of time.

2.2. Experimental set-up

The pyrolysis experiments were performed using a Stanton Red Croft Model 1500 thermobalance interfaced with a personal computer (PC) in order to record the temperature differences and weight loss during the reaction. The sensitivity of the thermobalance is about ± 0.1 mg. The thermobalance operates over a wide temperature range (20–1550°C) and for heating rates between 0.1 and 50°C min^{-1}.

Experiments were performed in a nitrogen stream of 20 ml min^{-1} in order to reduce the volatile product–solid interactions [1] and heat transfer resistances.

The furnace coil was composed of platinum–rhodium, and a platinum/platinum–rhodium thermocouple was located under the holder containing the sample in order to measure the differences ($\Delta T(t) = T_s(t) - T(t)$) between the sample and pyrolytic chamber temperatures as a function of the time t. In all the experiments, a sample of 50 mg of ASRs was used.

Calorimetric experiments were performed in a Rheometric Scientific PL-STA, which can perform calorimetric and thermogravimetric analysis simultaneously, in order to determine the reaction enthalpies.

3. Lumped kinetic model

The goal of the kinetic analysis is to achieve a simple kinetic model for the thermal decomposition of biomass, and to obtain the values of the corresponding kinetic rate, activation energies and reaction enthalpies. In the case of samples usually encountered in processing industrial wastes (ASRs),

it is almost impossible to determine a mechanistic reaction pathway from chemical considerations or to obtain, from a priori analysis, the values of the activation energies associated with each reaction, since the chemical compounds forming the solid mixture are unknown.

For this reason, the lack of structural and chemical composition data on the reactant, one of the most suitable ways to approach the problem is to make use of continuous kinetic modelling [14,15] by means of simplified semiempirical models.

Pyrolytic decomposition can be schematized as a set of parallel (independent) reactions occurring for the continuously lumped pseudo-components $\mathscr{C}_{E_a}$ (also referred to as key components), parametrized with respect to the activation energy E_a,

$$[\mathscr{C}_{E_a}] \rightarrow [\text{Volatiles}] + \gamma(E_a)\,[\text{Char}] \qquad (1)$$

where $\gamma(E_a)$ are the effective stoichiometric coefficients in the lumping.

Let M_0 and M_{inert} be the initial weights of the sample and the inert materials (glass, metallic oxides, etc.) respectively, $m(t; E_a)\,dE_a$ the mass fraction of the volatilizable compounds, i.e., the pseudo-components $\mathscr{C}_{E_a}$ possessing an activation energy between E_a and $E_a + dE_a$, and $x(t; E_a) = m(t; E_a)/(M_0 - M_{inert})$ the weight fraction in an inert-free basis.

The effect of the inert N_2 stream is to wash out the volatile products in order to prevent the occurrence of volatile-solid residue reactions which may be the cause of nonlinearities in the kinetics [1]. Therefore, by assuming first-order reactions (as discussed in Section 3), the decomposition kinetics of each pseudo-component is given by

$$\frac{\partial x(t; E_a)}{\partial t} = -k_0(E_a)\exp(-E_a/RT_s(t))\,x(t; E_a)$$
$$x(t; E_a)|_{t=0} = x_0(E_a) \qquad (2)$$

where $T_s(t)$ is the sample temperature, $k_0(E_a)$ is the kinetic rate and $x_0(E_a)$ is the initial fraction of the $\mathscr{C}_{E_a}$ pseudo-component.

In thermogravimetric experiments (differential temperature analysis), the difference $\Delta T(t) = T_s(t) - T(t)$ is measured, where $T(t)$ is the temperature in the pyrolytic chamber and $T_s(t)$ is the uniform reactant pellet temperature. In our experiments, the temperature oscillations for $\Delta T(t)$ are much smaller than for $T(t)$, $|\Delta T|(t) \ll T(t)$, which implies that $T_s(t)$ can be approximated by $T(t)$, which is externally forced according to a given temperature programme (linear temperature rise or constant temperature profiles). As it concerns heat transfer, the purging effect of the N_2 stream and the chosen granulometry (indeed ASRs are composed of a filamentous fluff) tend to diminish the heat transfer resistance. For this reason, heat transfer effects can be practically neglected in the present analysis, although it should be clear that this is a fairly crude model assumption. The experimental plausibility of this assumption can be checked using the data in Fig. 1B, by comparing the scales of the x and y axis, and a posteriori from the predictive capability of the model over a broad range of heating rates (5–45 K min^{-1}).

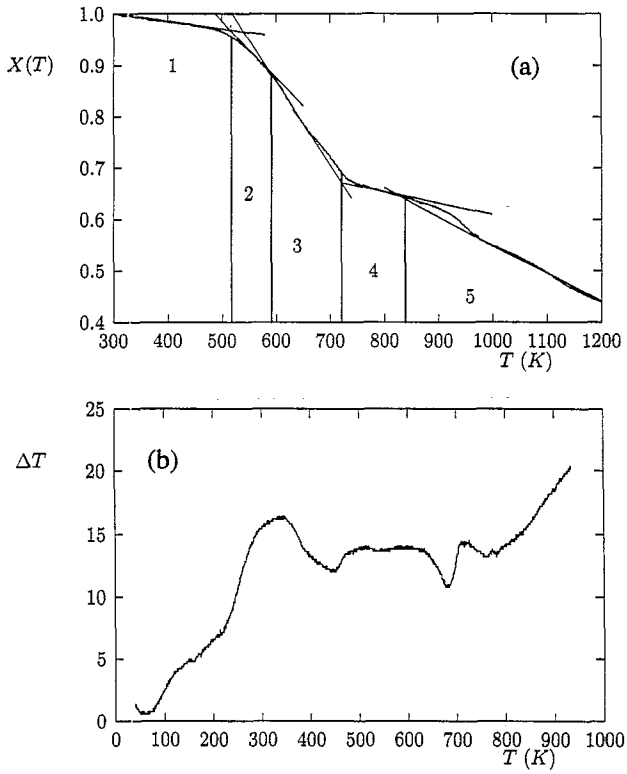

Fig. 1. (A) $X(T)$ vs. T in order to show qualitatively the subdivision into pseudo-components ($v_T = 5$ K min^{-1}). (B) Differential thermal analysis, ΔT vs. T, $v_T = 5$ K min^{-1}.

On the basis of this approximation, Eq. (2) can be solved analytically, because $T(t)$ is known, and gives

$$x(t; E_a) = x_0(E_a)\exp\left[-k_0(E_a)\int_0^t \exp(-E_a/RT(\tau))\,d\tau\right] \qquad (3)$$

Since ASRs contain a considerable amount of inert material (greater than 60 wt.%, see Table 1), it is convenient to represent the overall reaction kinetics with respect to an inert-free basis, in order to highlight the relevant scales, thus defining

$$X(t) = \frac{M(t) - M_{inert}}{M_0 - M_{inert}} \qquad (4)$$

The function $\gamma(E_a)$ is the specific char yield, also referred to as the effective stoichiometric coefficient. This means that $\gamma(E_a)\,[x_0(E_a) - x(t; E_a)]\,dE_a$ is the char fraction on an inert-free basis produced by the pseudo-component with an activation energy between E_a and $E_a + dE_a$.

According to the definition, $X(t)$ is the superposition of the volatilizable compounds not yet reacted and of the char formed due to Eq. (1), i.e.,

$$X(t)=\int_0^{\infty}x(t;E_a)\,dE_a+\int_0^{\infty}\gamma(E_a)\,[x_0(E_a)-x(t;E_a)]\,dE_a$$

$$=X_{c,\infty}+\int_0^{\infty}\tilde{x}_0(E_a)\exp\left[-k_0(E_a)\times\int_0^{t}\exp(-E_a/RT(\tau))\,d\tau\right]dE_a \quad (5)$$

where $X_{c,\infty}$ is the char fraction for $t\to\infty$

$$X_{c,\infty}=\frac{M_{char,\infty}}{M_0-M_{inert}}=\int_0^{\infty}\gamma(E_a)x_0(E_a)\,dE_a \quad (6)$$

and

$$\tilde{x}_0(E_a)=x_0(E_a)\,[1-\gamma(E_a)\,] \quad (7)$$

The choice of the optimal lumping strategy is to be guided by the experimental results. Indeed, differential temperature analysis (Fig. 1B) (the corresponding $X(T)$ vs. T diagram is depicted in Fig. 1A) suggests the presence of well-defined heat sources (algebraic meaning) due to endothermic/exothermic reactions localized at defined temperature intervals. The data in Fig. 1B reveal the presence of $N=5$ localized maxima/minima. This implies that the most convenient choice of kinetic lumping is given by an atomic initial distribution function $x_0(E_a)$

$$x_0(E_a)=\sum_{i=1}^{N}x_{0,i}\delta(E_a-E_i) \quad (8)$$

where $\sum_{i=1}^{N}x_{0,i}=1$, $E_i=E_{a,i}$ (E_i are ordered in an increasing way) and $N=5$. According to the discrete lumping (Eq. (8)), $\gamma(E_a)$ and $k_0(E_a)$ attain N values $\gamma_i=\gamma(E_i)$, $k_i=k_0(E_i)$, $i=1,\ldots,N$, and $\sum_{i=1}^{N}\gamma_i x_{0,i}=X_{c,\infty}$.

Therefore, the global kinetics can be given by the summation over the temporal evolutions of each pseudo-component

$$X(t)=X_{c,\infty}+\sum_{i=1}^{N}\tilde{x}_{0,i}\exp\left[-k_i\int_0^{t}\exp(-E_i/RT(\tau))\,d\tau\right] \quad (9)$$

where $\tilde{x}_{0,i}=x_{0,i}(1-\gamma_i)$.

Because the heating rate v_T is constant, $T(t)=T_0+v_T t$, Eq. (9) can be transformed into a temperature-dependent global behaviour as

$$X(T)=X_{c,\infty}+\sum_{i=1}^{N}\tilde{x}_{0,i}\exp\left[-k_i\Big/v_T\int_{T_0}^{T}\exp(-E_i/RT')\,dT'\right] \quad (10)$$

Let us discuss briefly the functional form of Eq. (9) in the light of parameter estimation. The overall kinetics is the linear superposition of the kinetics for each component $x_i(t)$. In the case of linear temperature profiles (constant heating rates), $x_i(t)$ depends on E_i through a nonlinear function $\int_0^t\exp(-E_i/RT(\tau))\,d\tau$. This functional dependence makes it difficult to obtain the parameters directly from the experimental data, without making use of brute-force optimization methods. We believe that the optimization step in complex kinetics should always be considered as an extreme ratio, and not as a rule, once all other theoretical approaches to determine the parameters in a smarter way fail. It should be noted that, in most of the literature on biomass thermal decomposition, brute-force parameter optimization has been extensively applied, this choice being forced in many cases by the complexity of the problem.

In principle, if the activation energies are sufficiently well separated, it is possible to decompose the timescale into several intervals, $I_i=[t_i,t_{i+1})$, $i=1,\ldots,5$, $t_1=0$, and to approximate the overall kinetics $X(t)$ on I_i with $x(t;E_i)$, i.e., $X(t)\simeq x_i(t)$, $t\in[t_i,t_{i+1})$. Under these conditions, parameter estimation can be performed in a fairly elegant and rigorous way. However, this approximation does not hold in practical applications, and other approaches should be sought. A rather convenient way to simplify the problem is to consider isothermal experiments as discussed in Section 4.

4. Experimental results

As pointed out in Section 3, a convenient way to extract information on kinetic parameters entering into a lumping scheme is to perform a series of isothermal experiments at different temperatures. By changing the temperature, it is possible to give prominence to a subreaction associated with a specific key component, and therefore to obtain, for each reaction, a relationship between the rate coefficients and the activation temperatures.

Experiments were carried out under asymptotically isothermal conditions, i.e., by letting the temperature $T(t)$ rise linearly to a given temperature $T*$, and then maintaining a constant temperature

$$T(t)=\begin{cases}T_0+v_T t & t\in[0,t^*)\\ T^* & t>t^*\end{cases} \quad (11)$$

where $t*=(T*-T_0)/v_T$ and $T_0=298$ K.

According to Eqs. (9) and (11), the evolution of the quantity $X(t)$ for $t>t*$ is given by

$$X(t)-X_{c,\infty}=\sum_{i=1}^{N}x_i{}^*\exp(-k_i t\exp(-E_i/RT^*)),\quad t>t^* \quad (12)$$

where x_i* is the value of $x_i(t)(1-\gamma_i)$ attained at $t=t*$. If the temperature $T*$ is chosen in such a way that only one key component, say j, can be isolated, because the remaining components have already reacted completely ($i<j$), or their activation energies are so high that at $T*$ the associated reac-

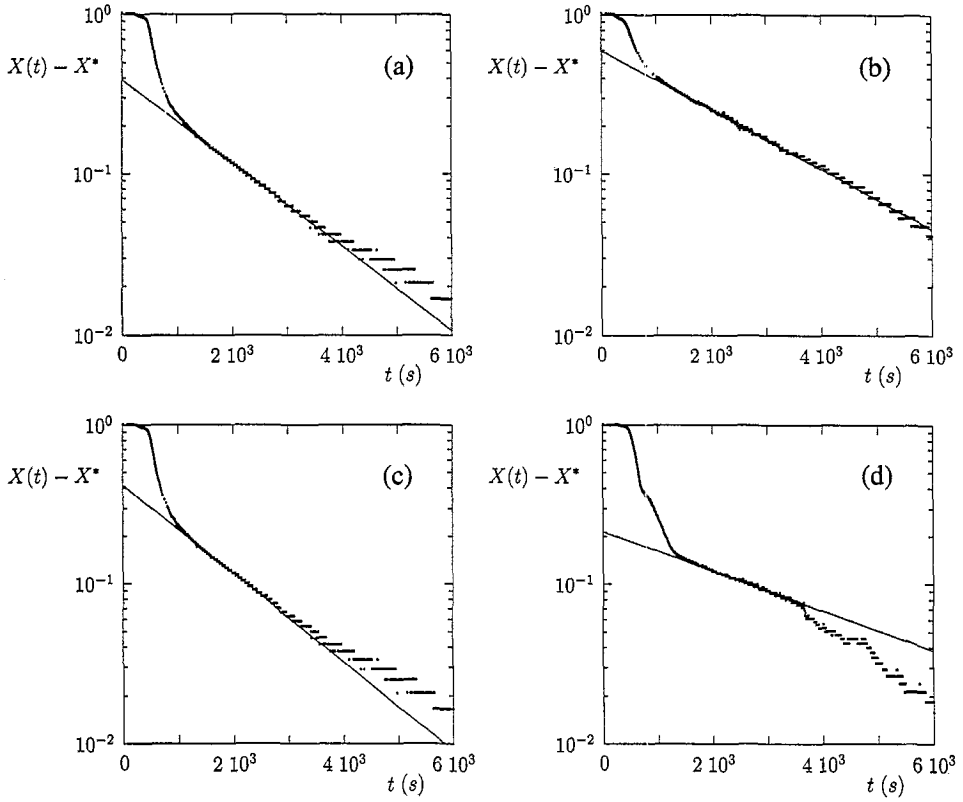

Fig. 2. $X(t)-X*$ vs. t (log–normal scale) for asymptotic isothermal thermogravimetric analysis ($\upsilon_T=5$ K min^{-1}). The vertical dotted lines show the value of $t=t*$ at which $T(t)$ reaches $T*$. Dots show the experimental data and the full lines the asymptotic regressions $\ln(X(t)-X*)=-\alpha_j t+B$. (a) $T*=573$ K; (b) $T*=663$ K; (c) $T*=873$ K; (d) $T*=973$ K.

tions practically do not proceed ($i>j$), Eq. (12) simplifies as

$$X(t)-X^* \simeq x_j^* \exp(-k_j t \exp(-E_j/RT^*)) \quad (13)$$

where $X*=X_{c,\infty}+\sum_{i>j}^{N} x_i*$; from the log–normal plot of $X(t)-X*$ vs. t it is possible to directly obtain the slope α_j

$$\alpha_j = k_j \exp(-E_j/RT^*) \quad (14)$$

$\log(X(t)-X*)\sim-\alpha_j t$, which can be regarded as a functional relation between k_j and E_j. By repeating the same procedure for different values of $T*$, a set of relationships between k_i and E_i are thus obtained for each key component.

Fig. 2(a)–(d) shows the behaviour of $\log(X(t)-X*)$ vs. t at different temperatures $T*$. The temperature $T*$ is chosen in such a way to highlight the asymptotic behaviour of each key component $i=1,\ldots,5$. The same analysis has also been performed for key component 1, but is not reported here, because component 1 is essentially related to moisture and bond-water evaporation.

An asymptotic exponential behaviour can be observed in Fig. 2(a)–(d), confirming the validity of the assumption of first-order kinetics.

Table 2 shows the values of α_i and $T*$ obtained from the analysis of asymptotically isothermal runs. Once the values of α_i have been determined, the remaining parameters can be estimated by standard optimization routines, by considering non-isothermal experiments. The initial choice of $\tilde{x}_{0,i}$ can be obtained directly from the non-isothermal behaviour, because the reaction shows sharp discontinuities corresponding to the extinction of one subreaction and the initiation of the next (see Fig. 1A). However, the values of $\tilde{x}_{0,i}$ need to be optimized, because they explicitly depend on the unknown parameters γ_i associated with char production. The set of conditions (Eq. (14)), derived from asymptotically isothermal runs, yields a system of strong constraints in the optimization. Because the α_i values are known, k_i can be expressed as a function solely of E_i, and the activation energy can be obtained fairly accurately on optimization. Kinetic (i.e., E_i) and structural (i.e., $\tilde{x}_{0,i}$) parameters have been estimated by considering a non-isothermal run at $\upsilon_T=5$ K min^{-1}. The comparison between model and experiment is shown in Fig. 3a.

Table 2
Review of the parameter values characterizing the model

Key component i	1	2	3	4	5
$\tilde{x}_{0,i}$	0.05	0.35	0.22	0.16	0.22
T_i* (K)	373	573	663	873	973
$\alpha_i\cdot10^5$ (s^{-1})	60.0	43.0	70.0	20.0	25.0
E_i/R (K)	1700.0	5300.0	5500.0	10000.0	12000.0

To check the validity of the model, we carried out other experiments at higher heating rates (see Fig. 3b–e). The model is fully predictive, because no parameter adjustments were performed. The agreement between the model and experiments is satisfactory when we consider the highly het-

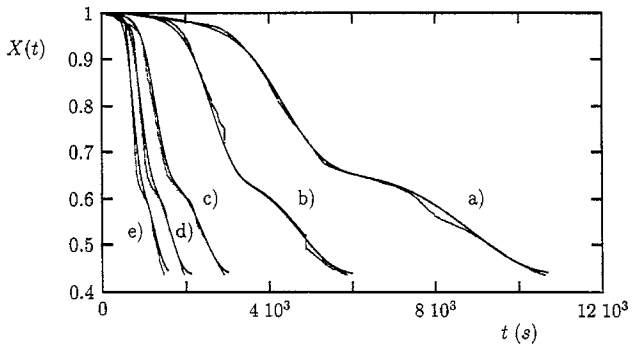

Fig. 3. Global kinetics $X(t)$ (with respect to an inert-free basis) vs. t. Dots represent the experimental data and full lines the model predictions. (a) $v_T = 5$ K min^{-1}; (b) $v_T = 10$ K min^{-1}; (c) $v_T = 20$ K min^{-1}; (d) $v_T = 30$ K min^{-1}; (e) $v_T = 45$ K min^{-1}.

Table 3
Reaction enthalpies ΔH_i associated with the key components

Key component i	1	2	3	4	5
ΔH_i (J g^{-1})	–	−111.43	33.61	251.12	95.65

erogeneous nature of ASRs. Moreover, the quantitative discrepancies between model and experiments fall in the same range (the large deviation is less than 4.0% and the mean deviation is less than 2.0%) as obtained in the kinetic analysis of other samples of biomass (see, for example, Ref. [7]), for which a more detailed chemical characterization is available.

The experimental set-up used in this research does not permit the on-line monitoring of char formation. Moreover, there are intrinsic difficulties in performing this task, and only the char content at the end of pyrolysis can be measured. In all the experiments, with heating rates ranging between 5 and 10 K min^{-1}, and for a maximum temperature of $T = 1200$ K, a char weight fraction $X_{c,\infty} = 0.42 \pm 0.02\%$ has been measured.

The reaction enthalpies associated with each key component, obtained from calorimetry, are reported in Table 3. For key component 1, ΔH is not reported, because it is essentially moisture and ΔH corresponds to its latent heat. It is interesting to observe that one reaction is exothermic (key component 2) and the others endothermic.

In summary, the experimental data support the initial assumption of a linear (first-order) thermal decomposition. The lumped model, despite its simplicity, can predict, with acceptable accuracy, the pyrolytic kinetics of ASRs over a broad range of temperatures.

5. Concluding remarks

In this article, we have analysed the pyrolysis kinetics of ASRs, which is a new field of thermal treatment for the reduction of the environmental impact of urban/industrial wastes.

A lumped kinetic model has been proposed, and shows a satisfactory agreement with experimental results over a broad range of temperatures and operating conditions. The model proposed is semiempirical, and linear decomposition kinetics have been assumed. This is a consequence of the lack of a detailed chemical characterization of ASRs, which is almost impossible to obtain in practice.

Isothermal runs provide a set of conditions (Eq. (14)) between rate coefficients (prefactors) and activation energies, and simplify considerably the parameter estimation of the remaining coefficients in the model. It is also important to stress that isothermal experiments furnish an experimental confirmation of the model, i.e., the assumption of linear first-order kinetics.

The kinetic analysis developed represents a first step towards the design of gasifiers for ASRs. The gasification kinetics and the development of design criteria for gasifiers for ASRs will be discussed elsewhere.

Finally, it is important to stress that the reducing conditions during pyrolysis inhibit the occurrence of side reactions producing noxious substances such as dioxin and polychlorobenzofurans. Therefore, the pyrolysis of ASRs can be viewed as an environmentally 'clean' process for the treatment of these wastes.

6. Nomenclature

E_a	activation energy (J mol^{-1})
E_i	$= E_{a,i}$ (J mol^{-1})
$k_0(E_a)$	rate coefficient (s^{-1})
k_i	$= k_0(E_i)$ (s^{-1})
$m(t; E_a)$	mass density function with respect to E_a (g mol J^{-1})
M	mass of the sample (g)
M_{inert}	mass of inert material (g)
M_0	initial mass (g)
$M_{char,\infty}$	mass of char formed at the end of pyrolysis (g)
N	number of pseudo-components (key components)
R	gas constant (J mol^{-1} K^{-1})
t	time (s)
T	pyrolytic chamber temperature (K)
T_s	sample temperature (K)
$T*$	constant temperature in asymptotically isothermal conditions (K)
v_T	heating rate (K min^{-1})
$x_{0,i}$	initial weight fraction in the discrete lumping
$x(t; E_a)$	$= m(t; E_a)/(M_0 - M_{inert})$ (mol J^{-1})
$x_0(E_a)$	initial weight fraction in the continuous lumping (mol J^{-1})
$\tilde{x}(E_a)$	$= x(E_a)[1 - \gamma(E_a)]$ (mol J^{-1})
$\tilde{x}_{0,i}$	$= x_{0,i}(1 - \gamma_i)$
$X(t)$	$= (M(t) - M_{inert})/(M_0 - M_{inert})$
$X_{c,\infty}$	$= M_{char,\infty}/(M_0 - M_{inert})$ char fraction formed at the end of pyrolysis

Greek letters

α_i	$=k_i\exp(-E_i/RT*)$ (s^{-1})
$\gamma(E_a)$	effective stoichiometric coefficient for char production
γ_i	$=\gamma(E_i)$
ΔH_i	reaction enthalpy
ΔT	$=T_s-T$ (K)

Subscripts

i	ith pseudo-component in the lumped kinetics

Acknowledgements

This work was partially supported by MURST 40% grants. The authors thank Ecofer for supporting the research and furnishing the samples of ASRs.

References

[1] M.J. Antal, G. Varhegyi, Ind. Eng. Chem. Res. 34 (1995) 703.
[2] D.S. Scott, J. Piskorz, Can. J. Chem. Eng. 62 (1984) 404.
[3] V. Cozzani, L. Petarca, L Tognotti, Fuel, 74 (1995) 903.
[4] A. Broido, M.A. Nelson, Combust. Flame, 24 (1975) 263.
[5] F. Shafizadeh, J. Anal. Appl. Pyrolysis, 3 (1982) 283.
[6] F. Shafizadeh, A.G. Bradbury, J. Appl. Polym. Sci.23 (1979) 1432.
[7] C.A. Koufopanos, G. Maschio, A. Lucchesi, Can. J. Chem. Eng. 67 (1989) 75.
[8] C.A. Koufopanos, N. Papayannakos, G. Maschio, A. Lucchesi, Can. J. Chem. Eng. 69 (1991) 907.
[9] P. Ahuja, S. Kumar, P.C. Singh, Chem. Eng. Technol. 19 (1996) 272.
[10] V. Cozzani, C. Nicolella, L. Petarca, M. Rovatti, L. Tognotti, Ind. Eng. Chem. Res. 34 (1995) 2006.
[11] Z. Shen, M. Day, J.D. Cooney, G. Lu, C.L. Briens, M.A. Bergougnou, Can. J. Chem. Eng. 73 (1975) 357.
[12] F. Tremblay, A. Charette, Can. J. Chem. Eng. 66 (1988) 86.
[13] S. Cooley, M.J. Antal, J. Anal. Appl. Pyrolysis, 14 (1988) 149.
[14] R. Aris, G.R. Gavalas, Philos. Trans. R. Soc. London, Ser. A 260 (1966) 351.
[15] A. Nigam, M. Neurock, M.T. Klein, Reconciliation of molecular detail and lumping: an asphaltene thermolysis example, in: G. Astarita, S.I. Sandler (Eds.), Kinetic and Thermodynamic Lumping of Multicomponent Mixtures, Elsevier, Amsterdam, 1991, pp. 181–206.